Int. J. Heat Mass Transfer. Vol. 29, No. 10, pp. 1487–1493, 1986
Printed in Great Britain

0017–9310/86 $3.00 + 0.00
Pergamon Journals Ltd.

Adjustment of a thermally-stratified fluid in a container with vertical through-flow

JAE MIN HYUN

Department of Mechanical Engineering, Korea Advanced Institute of Science & Technology, P.O. Box 150, Chong Ryang, Seoul, Korea

and

JAE CHUN HYUN†

Department of Chemical Engineering, University of California, Berkeley, California 94720, U.S.A.

(*Received* 20 *June* 1985 *and in final form* 20 *February* 1986)

Abstract—The adjustment process of a thermally-stratified fluid in a container in response to an imposed vertically upward through-flow, M_0, is investigated. Finite-difference numerical solutions to the time-dependent Navier–Stokes equations for a cylindrical container are obtained to verify the theoretical model of Rahm (*Int. J. Heat Mass Transfer* **29,** 1479–1485 (1986)). The numerical results are in close agreement with the theoretical predictions for the interior temperatures. During the transient phase, the vertical sidewall boundary layer transport grows, and the vertical extent of the boundary layer increases. In the steady state, the boundary layer transport carries most of the imposed through-flow M_0. The interior is virtually stagnant with near-linear stratification. Because of the dominance of the advective activities, the time scale for the overall adjustment process is substantially reduced below the diffusive time. It is demonstrated that, with a proper choice of M_0, this method can be utilized as an effective tool to produce a stably stratified fluid in the geophysical laboratory.

1. INTRODUCTION

AN OBVIOUS technique to produce a stably stratified fluid is to confine the fluid between two horizontal, thermally-conducting plates and apply a vertically stabilizing temperature contrast ΔT (hot above cold) across the fluid layer. The stratification is attained as a result of the conduction of heat through the fluid; in the final state, a vertically linear temperature profile is established. The adjustment time is the diffusive time $O(h^2/\kappa)$, h being the thickness of the fluid layer, κ the thermal diffusivity of the fluid. However, it should be emphasized that, for the conductive mechanism to prevail, the non-horizontal boundaries of the container, which separate the fluid from the environment at temperature T_e, have to be completely insulating. In practice, this requirement of having perfectly insulating non-horizontal boundaries places a stringent condition for the experimental apparatus. Therefore, the determination of buoyant motions of a stratified fluid induced by the thermal forcing at the non-horizontal boundaries poses a problem of considerable concern in the laboratory.

Recently, Walin and Rahm [1–4] suggested an efficient way of stratifying a contained fluid. First, they allowed the non-horizontal boundaries to be incomplete insulators. Second, a small upward vertical mass flux M_0, whose temperature at the bottom inlet was controlled, was pumped through the porous horizontal boundaries. They developed the theory under several conditions, which were relevant to typical laboratory situations. Based on elaborate scaling arguments and boundary layer analyses, they successfully derived a one-dimensional differential equation for the lowest-order interior temperature. The crux of this model is that, by introducing the through-flow in the container, convection becomes an important factor in the determination of the interior stratification. Accordingly, the adjustment time is substantially reduced below the diffusive time scale. Also, the strict requirement of having perfectly insulating, non-horizontal boundaries has been relaxed. In effect, this model exploits the incomplete insulation of the non-horizontal boundaries as a means to control the interior stratification. For the simple geometry of a circular cylindrical container, approximate analytical solutions for the interior temperature were given: Rahm [4] examined the transient behavior, and Rahm and Walin [2, 3] illustrated the steady-state features. The steady-state temperature profiles were shown to agree well with the preliminary laboratory measurements.

The model proposed by Walin and Rahm offers a significant new idea for the laboratory techniques to produce stratified fluids. It is also important that this model sheds light on the basic nature of thermal adjustment of a stratified fluid system when the non-horizontal boundaries have finite thermal conductance. The theoretical foundation expounded by Walin and Rahm provides an ideal ground for numerical experiments. It is our purpose in these numerical experiments to verify the theoretical predictions.

In this paper, we acquired numerical solutions to

† On sabbatical leave from Tong Yang Cement Corporation, Seoul, Korea.

NOMENCLATURE

a	cylinder radius
A_0	cross sectional area
d	thickness of the sidewall
g	gravity
h	cylinder height
k	thermal conductivity
M_B	boundary layer transport
M_0	through-flow
N	buoyancy frequency [$\equiv (\alpha g \Delta T/h)^{1/2}$]
Pr	Prandtl number
r	radial coordinate
R	scaled radial coordinate [$\equiv r/a$]
Ra	Rayleigh number [$\equiv \alpha g \Delta T h^3/\nu\kappa$]
s	sidewall thermal conductance
t	time
ΔT	characteristic temperature difference
u,w	velocity component in (r, z) direction
z	vertical coordinate.

Greek symbols

α	coefficient of volumetric expansion
θ	nondimensional temperature
κ	thermal diffusivity
ν	kinematic viscosity
ρ	density
τ	characteristic time
ψ	stream function.

the time-dependent Navier–Stokes equations to describe the flow of a thermally-stratified, contained fluid with vertical through-flow. For maximal geometrical simplicity, we adopted a circular cylindrical container whose axis is parallel to gravity g. This also allowed us to conduct explicit comparisons with the available theoretical predictions.

In this paper, we present the results of both the transient evolution and the steady state flows which arise in response to an impulsive start of the vertical through-flow. We note that the transient behavior is of considerable interest to geophysical fluid modelling and to certain industrial applications [4]. The numerical approaches enable us to depict the flow details, which may not be readily available in laboratory measurements. The reader is referred to Fig. 1 for a definition sketch of flow configuration.

The numerical results exhibit satisfactory agreement with the theoretical predictions for the interior temperature. Physical descriptions of the development of flow and temperature fields are provided. Discussion will be focused on the effect of the magnitude of the through-flow on the flow structures. The numerical results demonstrate that, with a proper choice of the through-flow, a virtually motionless interior with near-linear stratification can be obtained. The time needed to reach the steady state is much smaller than the diffusive time scale. These results are clearly supportive of the contentions of the theory.

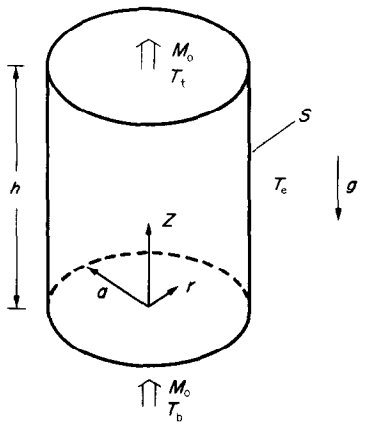

FIG. 1. Sketch of flow configuration.

2. THE MODEL

Consider a cylindrical container defined by $r \leqslant a$, $0 \leqslant z \leqslant h$, filled with a Boussinesq fluid, where a is the radius and h the height of the cylinder, and (r, z) denote the radial and vertical coordinates. At the initial state, the fluid is at rest with a prescribed linear temperature profile $T_i(z)$. At $t = 0$, an upward vertical through-flux M_0 is forced to pass through the porous horizontal endwall disks and is maintained so thereafter. The endwalls are thermal conductors with temperature T_b at the bottom inlet disk at $z = 0$ and T_t at the top outlet disk at $z = h$. Note that $\Delta T = T_t - T_b > 0$ for a gravitationally stable configuration. At the vertical sidewall, a Newtonian heat flux condition is applied:

$$\frac{\partial T}{\partial r} = s(T_e - T) \quad \text{at } r = a, \tag{1}$$

where T_e is the temperature of the environment. Here, the thermal conductance at the sidewall is represented by s. Physically, $s = k_w/kd$, where k_w and k denote the thermal conductivity of the wall material and of the fluid, and d the thickness of the wall [1]. In this study, we shall take s = constant in the ensuing discussion.

Based on boundary layer analyses and scaling arguments, Walin and Rahm [1–4] arrived at a one-dimensional differential equation for the lowest-order interior temperature T^I. This equation, written in nondimensional form, is (see equation (5) of Ref. [4])

$$\frac{\partial \theta^I}{\partial t'} + A_r \frac{\partial \theta^I}{\partial z'} + B_r(\theta^I - \theta_e) = C_r \frac{\partial^2 \theta^I}{\partial z'^2}, \tag{2}$$

in which we introduced the following nondimensional quantities:

$$z' = z/h, \quad t' = t/\tau, \quad \theta = (T-T_b)/(T_t-T_b),$$
$$A_r \equiv M_0\tau/\pi a^2 h, \quad B_r \equiv 2\kappa\tau s/a, \quad C_r \equiv \kappa\tau/h^2. \quad (3)$$

In expressions (3), τ is the characteristic time scale of the adjustment process, which is yet to be determined. Physically, the coefficients A_r, B_r and C_r in equation (2) can be interpreted respectively as the ratio of the characteristic time to the flush time due to the imposed through-flow M_0, to the flush time due to the buoyancy layer transport M_B, and to the diffusive time (see Rahm [4]). Here, we are concerned with the advection-dominant regime. Therefore, the time scale for the overall adjustment process is mainly governed by the flush time due to the boundary layer transport. This consideration leads to $\tau \sim a/(2\kappa s)$ so that $B_r \sim 1$ and $C_r \ll 1$ in equation (2). It follows that, since M_0 and M_B are comparable in magnitude, we have $A_r \sim O(1)$, pointing to $M_0 \gg \kappa A_0/h$.

Rahm [4] noted the smallness of C_r in equation (2) and considered a further simplification of mathematical analysis. A clear and informative account of the qualitative behavior of the fluid system is given in the companion paper [4].

This theoretical model is now subject to verification by numerical experiments.

3. THE NUMERICAL COMPUTATIONS

3.1. *Governing equations*

The governing incompressible Navier–Stokes equations for a Boussinesq fluid on a cylindrical frame are

$$\frac{\partial u}{\partial t} = -\frac{1}{r}\frac{\partial}{\partial r}(ru^2) - \frac{\partial}{\partial z}(uw) - \frac{1}{\rho_r}\frac{\partial p}{\partial r} + \nu\left(\nabla^2 u - \frac{u}{r^2}\right), \quad (4)$$

$$\frac{\partial w}{\partial t} = -\frac{1}{r}\frac{\partial}{\partial r}(ruw) - \frac{\partial}{\partial z}(w^2) - \frac{1}{\rho_r}\frac{\partial p}{\partial z} + \alpha g(T-T_r) + \nu\nabla^2 w, \quad (5)$$

$$\frac{\partial T}{\partial t} = -\frac{1}{r}\frac{\partial}{\partial r}(ruT) - \frac{\partial}{\partial z}(wT) + \kappa\nabla^2 T, \quad (6)$$

$$\frac{1}{r}\frac{\partial}{\partial r}(ru) + \frac{\partial w}{\partial z} = 0, \quad (7)$$

where

$$\nabla^2 = \frac{1}{r}\frac{\partial}{\partial r}r\frac{\partial}{\partial r} + \frac{\partial^2}{\partial z^2};$$

(u, w) are the velocity components in the (r, z) direction, respectively; t the time; p the reduced pressure; and T the temperature. The relevant fluid properties are ν, kinematic viscosity; κ, thermal diffusivity; α, coefficient of volumetric expansion. The equation of state is

$$\rho = \rho_r[1-\alpha(T-T_r)], \quad (8)$$

in which ρ is density, and subscript r denotes the reference values.

3.2. *Initial and boundary conditions*

At the initial state, the fluid was at rest with a prescribed linear temperature profile:

$$u = w = 0, \quad T = T_i(z) \quad \text{at } t = 0. \quad (9)$$

At $t = 0$, a vertical through-flow, M_0, was forced to pass through the porous, thermally-conducting, horizontal endwall disks; and this through-flow was maintained so thereafter:

$$\begin{aligned} &u = 0, \quad w = M_0/\pi a^2, \quad t = T_b \quad \text{at } z = 0, \\ &u = 0, \quad w = M_0/\pi a^2, \quad T = T_t \quad \text{at } z = h. \end{aligned} \quad (10)$$

As was discussed in equation (1), the conditions at the vertical sidewall were

$$u = w = 0, \quad \partial T/\partial r = s(T_e - T) \quad \text{at } r = a. \quad (11)$$

3.3. *Computations performed*

The finite-difference numerical model of Warn-Varnas *et al.* [6] was amended to apply to the present problem. The governing equations and the boundary conditions were written in finite-difference form using a staggered mesh. A non-uniform grid was adopted in order to have adequate resolution of the flows in the boundary layers. The reliability and accuracy of this numerical procedure has been validated previously for a variety of time-dependent, stratified flows by checking the model predictions against laser-Doppler velocimeter measurements (see, e.g. Hyun *et al.* [7]).

Numerical computations were performed using the following values for the physical parameters: $a = 3$ cm, $h = 7$ cm, $\alpha = 2.86\times10^{-4}\,^{\circ}\mathrm{C}^{-1}$, $\nu = \kappa = 8.3\times10^{-3}$ cm^2 s^{-1}, $\Delta T = 10^{\circ}$C, $s = 1.5$ cm^{-1}, which gave $Ra = 1.40\times10^7$, $Pr = 1.0$, $Nh^2/\nu = 3.7\times10^3$, $sh = 10.5$. These nondimensional numbers were consistent with the basic assumptions pertinent to the theory [1–4], i.e. $Ra \gg 1$, $Pr \sim O(1)$, $Nh^2/\nu \gg 1$, $sh \ll (\kappa/Nh^2)^{-1/2}$. The vertical sidewall can be made of glass about 1 cm thick to simulate these numerical experiments [1]. In the present study, we took T_e to be the mean of T_b and T_t, i.e. $\theta_e = 0.5$.

In accordance with the conditions for the advection-dominated regime, as was set forth in equation (2), we designed our experiments with $\tau = 120$ s, which would correspond to $B_r = 1.0$, $C_r = 0.02$. Three specific cases were calculated in order to reveal the effect of the magnitude of the through-flow M_0 on the adjustment process:

Case C1, $M_0 = 0.66\,\mathrm{cm}^3\,\mathrm{s}^{-1}$ [$A_r \approx 0.4$];

Case C2, $M_0 = 1.65\,\mathrm{cm}^3\,\mathrm{s}^{-1}$ [$A_r \approx 1.0$];

Case C3, $M_0 = 8.25\,\mathrm{cm}^3\,\mathrm{s}^{-1}$ [$A_r \approx 5.0$].

The initial temperature profile was taken as $\theta_i(z) = 0.3 + 0.6z/h$. Rahm [4] adopted this exemplary profile in his numerical integration of equation (2).

3.4. *Run-time information*

Finite-difference numerical solutions to the time-dependent Navier–Stokes equations were obtained using a (22×22) grid in the (r, z) plane. The sensitivity of the results of this numerical model to grid size was tested by Warn-Varnas *et al.* [6]. The time step used was $\Delta t = 0.05 \sim 0.10$ s. The time-marching integration continued up to about 2τ. As will be seen later, this time was typically beyond the point of an almost complete (say, 99%) attainment of the steady state. The computer time was approximately $1\frac{1}{2} \sim 2$ h on an IBM 4341 computer, depending on the cases calculated.

4. RESULTS AND DISCUSSION

This section presents the results of the numerical experiments. In order to verify the theoretical predictions for the interior temperature, a separate numerical integration of equation (2) was performed using the specified values of A_r, B_r, C_r. Equation (2), which is a one-dimensional, unsteady equation for θ^I, was solved by the Crank–Nicolson method.

Figure 2 shows the vertical profile of temperature along $R[\equiv r/a] = 0.5$ for Case C2. The plots of isotherms in the (r, z) plane indicate that the temperature variations in the horizontal direction are minimal throughout the flow field except within the thin boundary layer on the sidewall. The horizontal uniformity of the interior temperature is a well-known property in stratified fluids. Therefore, the profiles displayed in Fig. 2 are representative of the temperature structure in the entire interior region. It is apparent in Fig. 2 that the adjustment process is substantially completed over the time span $O(\tau)$ (the temperature field approaches the steady state at $t' = 1.41$ for Case C2). Here, the steady state is arbitrarily defined as the state when the maximum temporal variation of temperature drops below 0.1% over the time period of 0.1τ. Figure 2 clearly demonstrates close agreement between the numerical results and the theoretical solutions to equation (2).

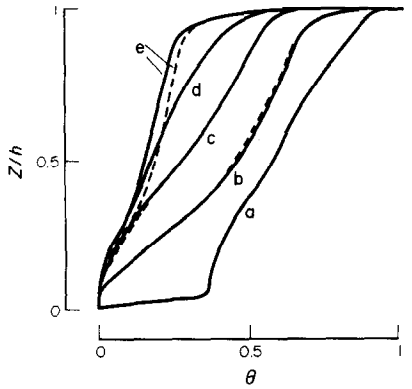

FIG. 2. Temperature profiles along $r/a = 0.5$ for Case C2. ——, numerical results; – – –, theoretical predictions [equation (8)]. Times are (a) $t' = 0.01$, (b) $t' = 0.24$, (c) $t' = 0.50$, (d) $t' = 0.76$, (e) show the steady state, $t' \geq 1.30$ (——), $t' \geq 1.41$ (– – –).

The fluid near the inlet disk adapts quickly to the imposed boundary conditions. Consequently, during the principal phase of the transient process, the temperature condition at the bottom inlet, i.e. $T = T_b$ at $z = 0$, is satisfied by the interior temperature itself. On the other hand, near the outlet disk, the interior temperature cannot meet the boundary condition, i.e. $T = T_t$ at $z = h$. A boundary layer is needed near the outlet disk to accommodate the interior temperature to T_t. Rahm and Walin [2] pointed out that this boundary layer is passive and it does not control the interior dynamics.

Figure 3 illustrates the time-dependent flow field for Case C2. We have constructed the plots of stream function ψ, which is defined such that $u = (1/r)(\partial\psi/\partial z)$, $w = -(1/r)(\partial\psi/\partial r)$. No explicit analytical expressions for the velocity field were given in the theory. Therefore, no direct comparisons with the theoretical solutions were attempted.

At early times, the cold fluid brought in by the through-flow has not penetrated into the main part of the container. Therefore, as is observable in Fig. 2, in the bulk of the container, $|\theta_c - \theta^I|$ is small and $\partial\theta^I/\partial z$ is large. These imply that the boundary layer transport remains to be small (see equation (3) of Ref. [4]). Consequently, the vertical fluid transport takes place principally throughout the interior [see Fig. 3(a)]. At intermediate times, the cold fluid of the through-flow has advanced to the mid-levels of the container. Ahead of the advancing front of the cold fluid, the vertical

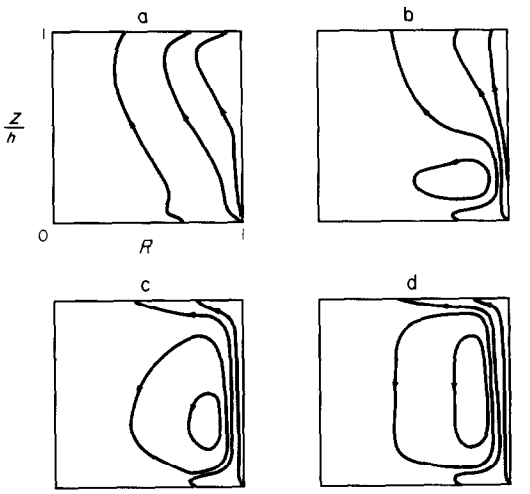

FIG. 3. Numerical results for stream function ψ for Case C2. $\Delta\psi$ denotes the contour increment. Values of ψ are shown in $cm^3\,s^{-1}$. (a) $t' = 0.17$, $\psi_{max} = 0$, $\psi_{min} = -0.327$, $\Delta\psi = 0.1$; (b) $t' = 0.54$, $\psi_{max} = 0.129$, $\psi_{min} = -0.265$, $\Delta\psi = 0.1$; (c) $t' = 1.07$, $\psi_{max} = 0.191$, $\psi_{min} = -0.262$, $\Delta\psi = 0.1$; (d) $t' = 1.75$, $\psi_{max} = 0.200$, $\psi_{min} = -0.262$, $\Delta\psi = 0.1$.

fluid motion is spread over the interior. However, behind the front, due to the influence of the cold fluid brought in by the through-flow, $|\theta_e - \theta^I|$ now becomes appreciable, and $\partial\theta^I/\partial z$ becomes smaller (see Fig. 2). These point to enhanced sidewall boundary layer transport in the upstream region; in the interior, the vertical flows are reduced in magnitude accordingly. The mass flux carried by the boundary layer transport cannot continue into the region ahead of the front; the fluid enters into the interior near the level of the front. In the region between the front and the inlet disk, a weak counter-clockwise circulation is formed in the interior [see Fig. 3(b)]. At a still later time, the front has advanced further toward the outlet disk. The region between the front and the inlet disk has expanded, and the flow patterns described above prevail more strongly in this region [see Fig. 3(c)]. As can be seen in Fig. 2, $|\theta_e - \theta^I|$ in the bulk of the flow field has increased, $\partial\theta^I/\partial z$ becomes even smaller; the boundary layer transport has intensified. In the steady state, in the main part of the container, the boundary layer transport substantially carries the vertical mass flux. The vertical motions in the main part of the interior have diminished. Only in a narrow region adjacent to the outlet disk, a boundary layer exists to adjust the flow to the imposed boundary conditions at the outlet. In summary, in the bulk of the container, we have achieved a virtually motionless, near-linear stratification. As was emphasized earlier, this process is accomplished over $O(\tau)$, which is substantially shorter than the diffusive time scale. The salient features of the transient flows, as depicted in Figs. 2 and 3, are consistent with the qualitative descriptions provided by Rahm [4].

Figures 4 and 5 display the results for Case C1. These show the effect of decreasing through-flow [$A_r = 0.4$ for Case C1] on the flow patterns. The agreement between the numerical results and the theoretical predictions for θ^I remains to be satisfactory. As anticipated, the overall advective activities are reduced in magnitude, as M_0 decreases. Since the effect of the imposed through-flow is small, the relative importance of the sidewall thermal forcing grows. Figure 4 shows that $|\theta_e - \theta^I|$ is smaller and $\partial\theta^I/\partial z$ is larger than for the case of C2, pointing to a reduced boundary layer transport for Case C1 (see equation (3) of Ref. [4]). Also, the time needed to reach the steady state

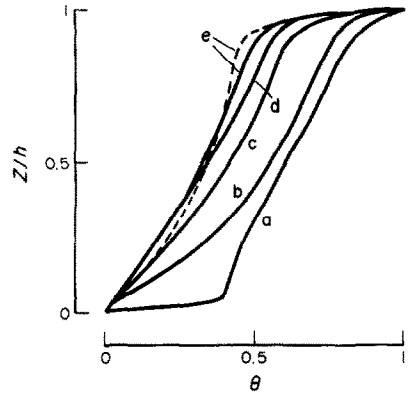

FIG. 4. Same as in Fig. 2, except for Case C1. (a) $t' = 0.014$, (b) $t' = 0.27$, (c) $t' = 0.82$, (d) $t' = 1.27$. For curves (a)–(d), the numerical results and the theoretical predictions almost overlap for graphical presentation. (e) $t' = 1.72$ (——), $t' \geqslant 2.58$ (– – – –).

becomes larger ($t' = 2.58$ for Case C1), although the overall transient phase is still characterized by $O(\tau)$.

At early times, the boundary layer transport is minimal, and the vertical fluid transport takes route principally via the interior. However, in most of the upper region near the sidewall, θ_e is considerably lower than θ^I. Since the relative importance of the sidewall forcing is more pronounced, an appreciable cooling of the fluid in the boundary layer in this region takes place. A sinking motion in the upper part of the boundary layer results, which drives a clockwise circulation in the upper corner area [see Fig. 5(a)].

At intermediate times, the cold fluid of the through-flow occupies a wider portion of the container, reducing the magnitude of $\partial\theta^I/\partial z$. In the upstream region, the upward fluid transport by the boundary layer increases, which induces a counter-clockwise circulation in the interior. In the downstream region, the sinking motion in the upper part of the boundary layer weakens accordingly [see Fig. 5(b)].

As time progresses toward the steady state, in the main region of the container, the upward fluid transport by the boundary layer intensifies and weak downward flows exist in the interior. However, since the advective activities due to the through-flow are less vigorous, the clockwise circulation near the upper corner persists, although it is weak and confined to a small area.

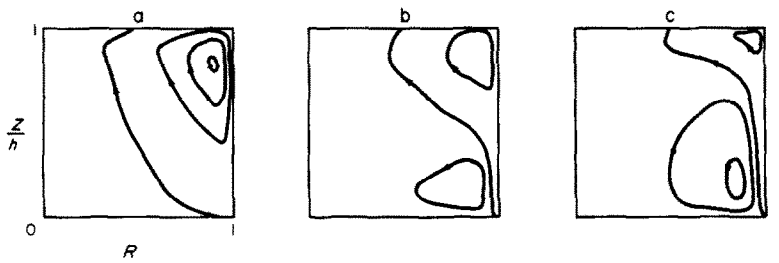

FIG. 5. Same as in Fig. 3, except for Case C1. (a) $t' = 0.14$, $\psi_{max} = 0$, $\psi_{min} = -0.211$, $\Delta\psi = 0.06$; (b) $t' = 0.81$, $\psi_{max} = 0.076$, $\psi_{min} = -0.124$, $\Delta\psi = 0.06$; (c) $t' = 1.72$, $\psi_{max} = 0.099$, $\psi_{min} = -0.111$, $\Delta\psi = 0.06$.

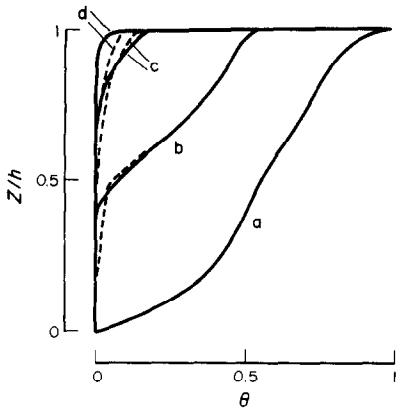

FIG. 6. Same as in Fig. 2, except for Case C3. (a) $t' = 0.02$, (b) $t' = 0.13$, (c) $t' = 0.23$, (d) $t' \geqslant 0.49$ (——), $t' \geqslant 0.40$ (– – – –).

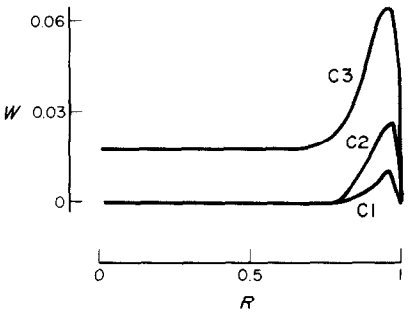

FIG. 8. Radial profile along $z/h = 0.5$ of the steady-state vertical velocity. Units are in cm s^{-1}.

In summary, as M_0 decreases, the overall intensity of the interior flows decreases accordingly. The steady-state interior temperature distribution tends to a near-linear profile over much of the container. In the limit $M_0 = 0$, Hyun [8] showed that the steady-state velocity field is characterized by two oppositely-directed circulation cells of comparable strength, and that the interior fluid approaches a linear stratification.

Figures 6 and 7 pertain to Case C3, exemplifying the flow patterns when the effect of the through-flow is large [$A_r = 5.0$ for C3]. Since the imposed through flow is quite vigorous, the cold fluid brought in by the through-flow quickly replaces the original fluid in the container. The interior temperature evolution is dominated by the through-flow. The overall adjustment time becomes smaller; the steady state is reached at $t' = 0.40$ for Case C3. In the steady state, the interior temperature in much of the container is fairly close to the temperature of the through-flow. Near the outlet disk, a boundary layer exists to adjust the interior temperature to the boundary temperature T_t. The dominant influence of the through-flow on the velocity field is apparent in Fig. 7. The sidewall boundary layer transport is vigorous and it carries most of the vertical fluid transport.

Figure 8 shows the radial profile of the steady-state vertical velocity along the mid-depth of the cylinder ($z/h = 0.5$). Concentration of the vertical flows in the sidewall boundary layer is evident. The vertical flows in the interior are fairly uniform and quite suppressed. Figure 8 suggests that if $A_r \lesssim O(1)$, the interior is virtually stagnant. If we desire an almost quiescent fluid with near-linear stratification, the method of Walin and Rahm can provide an effective laboratory technique to this end.

5. CONCLUSION

The numerical solutions to the Navier–Stokes equations have confirmed the correctness of the theory of Walin and Rahm. The transient behavior is heavily influenced by buoyant convective activities. The time scale for the overall adjustment process is much smaller than the diffusive time.

It has been demonstrated that, by a suitable choice of the through-flow M_0, a virtually stagnant fluid with near-linear stratification can be produced. The imperfect insulation at the vertical sidewall boundary is now utilized as a means to control the interior stratification.

Acknowledgement—Part of this work was conducted while the first author was on the faculty of Clarkson University in Potsdam, New York.

REFERENCES

1. G. Walin, Contained non-homogeneous flow under gravity or how to stratify a fluid in the laboratory, *J. Fluid Mech.* **48,** 647–672 (1971).
2. L. Rahm and G. Walin, Theory and experiments on the control of the stratification in almost-enclosed regions, *J. Fluid Mech.* **90,** 315–325 (1979).

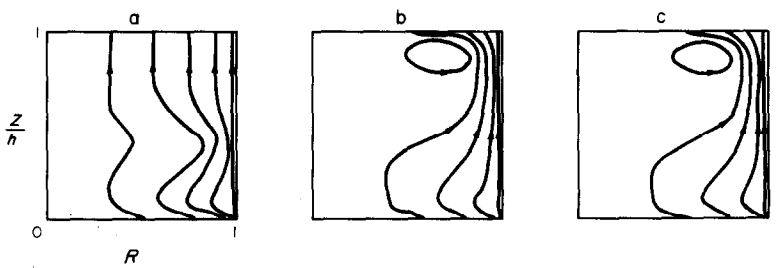

FIG. 7. Same as in Fig. 3, except for Case C3. (a) $t' = 0.13$, $\psi_{max} = 0$, $\psi_{min} = -1.31$, $\Delta\psi = 0.30$; (b) $t' = 0.36$, $\psi_{max} = 0.327$, $\psi_{min} = -1.31$, $\Delta\psi = 0.40$; (c) $t' = 0.66$, $\psi_{max} = 0.319$, $\psi_{min} = -1.31$, $\Delta\psi = 0.40$.

3. L. Rahm and G. Walin, On thermal convection in stratified fluids, *Geophys. Astrophys. Fluid Dyn.* **13,** 51–65 (1979).
4. L. Rahm, On the thermal adjustment of an almost enclosed fluid region with through-flow, *Int. J. Heat Mass Transfer* **29,** 1479–1485 (1986).
5. J. M. Hyun, Transient process of thermally stratifying an initially homogeneous fluid in an enclosure, *Int. J. Heat Mass Transfer* **27,** 1936–1938 (1984).
6. A. Warn-Varnas, W. W. Fowlis, S. Piacsek and S. M. Lee, Numerical solutions and laser-Doppler measurements of spin-up, *J. Fluid Mech.* **85,** 609–639 (1978).
7. J. M. Hyun, W. W. Fowlis and A. Warn-Varnas, Numerical solutions for the spin-up of a stratified fluid, *J. Fluid Mech.* **117,** 71–90 (1982).
8. J. M. Hyun, Flow of a stratified fluid bounded by walls of finite thermal conductance, *Geophys. Astrophys. Fluid Dyn.* **33,** 109–121 (1985).

AJUSTEMENT D'UN FLUIDE STRATIFIE THERMIQUEMENT DANS UN RESERVOIR AVEC UN ECOULEMENT VERTICAL DE TRAVERSEE

Résumé—On étudie le mécanisme d'ajustement d'un fluide thermiquement stratifié dans un réservoir, en réponse à un écoulement de traversée vertical ascendant M_0. Des solutions numériques aux différences finies des équations de Navier–Stokes pour un réservoir cylindrique sont obtenues pour vérifier le modèle théorique de Rahm[4]. Les résultats numériques sont en bon accord avec les prévisions théoriques des températures internes. Pendant la phase variable, le transport vertical dans la couche limite pariétale croît, et l'extension verticale de la couche limite augmente. En régime permament, le transport de couche limite emporte la plupart de l'écoulement imposé M_0. L'intérieur est virtuellement stagnant avec une stratification presque linéaire. A cause de la dominance des activités d'advection, l'échelle de temps pour le mécanisme global d'ajustement est fortement réduit en dessous du temps de diffusion. On montre qu'avec un choix approprié de M_0, cette méthode peut être utilisée comme un outil avantageux pour produire un fluide stratifié stable dans un laboratoire de géophysique.

EINSTELLUNG DES TEMPERATURFELDES IN EINEM THERMISCH GESCHICHTETEN FLUID IN EINEM BEHÄLTER BEI VERTIKALER DURCHSTRÖMUNG

Zusammenfassung—Es wird die Ausbildung eines Temperaturfeldes untersucht, das sich ergibt, wenn ein thermisch geschichtetes Fluid in einem Behälter durch eine vertikale Aufwärtsströmung, M_0, beeinflußt wird. Zur Nachbildung des theoretischen Modells von Rahm [4] werden numerische Lösungen der zeitabhängigen Navier–Stokes-Gleichungen für einen zylindrischen Behälter ermittelt. Für die Temperaturen im Inneren stimmen die numerischen Ergebnisse gut mit theoretischen Vorhersagen überein. Im instationären Zustand wächst der Transport in der Grenzschicht an der vertikalen Seitenwand, und die vertikale Erstreckung der Grenzschicht wird größer. Im stationären Zustand transportiert die Grenzschicht einen Großteil des aufgezwungenen Durchflusses M_0. Im Innern des Behälters stagniert die Flüssigkeit mit fast-linearer Schichtung. Wegen der Dominanz der advektiven Vorgänge sinkt die Einstellzeit für den Gesamtvorgang unter diejenige bei reiner Diffusion ab. Es wird gezeigt, daß bei einer geeigneten Wahl von M_0 diese Methode als ein nützliches Hilfsmittel verwendet werden kann, um ein stabil geschichtetes Fluid in einem geophysikalischen Labor darzustellen.

УСТАНОВЛЕНИЕ СТАЦИОНАРНОГО РЕЖИМА В ЖИДКОСТИ С ТЕПЛОВОЙ СТРАТИФИКАЦИЕЙ В ПОЛОСТИ С ВЕРТИКАЛЬНЫМ СКВОЗНЫМ ТЕЧЕНИЕМ

Аннотация—Исследуется процесс установления стационарного режима в жидкости с тепловой стратификацией при наложении вертикального направленного вверх сквозного течения, M_0. Для проверки теоретической модели Рама [4] получены численные конечно-разностные решения нестационарных уравнений Навье–Стокса для цилиндрической полости. Численные расчеты для температуры близки к теоретическим. В переходном режиме перенос в пограничном слое на векртикальной боковой стенке и толщина пограничного слоя в вертикальном направлении растут. В стационарном режиме перенос в пограничном слое становится доминирующим. Внутренняя область практически застойна с почти линейной стратификацией. Вследствие действия подъемных сил времена установления стационарного режима меньше времени диффузии. Показано, что при надлежащем подборе M_0 этот метод эффективен для получения устойчиво стратифицированной жидкости в геофизической лаборатории.